Available online at www.sciencedirect.com
ScienceDirect
Ceramics International 36 (2010) 231–239
CERAMICS INTERNATIONAL
www.elsevier.com/locate/ceramint

Elaboration of porous mullite-based materials via SHS reaction

A. Esharghawi, C. Penot, F. Nardou *

SPCTS, CNRS, UMR 6638, Université de Limoges, 123 Avenue Albert Thomas, 87060 Limoges Cedex, France

Received 14 June 2009; received in revised form 30 June 2009; accepted 23 July 2009
Available online 25 August 2009

Abstract

In order to produce cheaper mullite from kaolinitic clays we worked on the opportunity to use self-propagating high-temperature synthesis (SHS) reaction to obtain this phase. Two ways were explored during the combustion of metals mixed with the clay. The first one concerns the nature of the combustion gas (air or pure oxygen) which was tested on mixtures of clay and metal powders. The second one showed the influence of magnesium addition in clay/Al mixture. Results conclude that to obtain porous mullite at low-cost by SHS process the best conditions are the addition of magnesium powder and combustion in oxygen gas. Because a SHS reaction is always quicker, we compared this process with the traditional reactive sintering in order to explain the structure and the microstructure of the SHS products.

Keywords: B. Porosity; D. Mullite; D. Clays; SHS process; Metal addition

1. Introduction

Due to its good physical properties [1–4] (low thermal expansion coefficient, low conductivity, good thermal stability, high creep resistance, etc.), mullite ($3Al_2O_3{\cdot}2SiO_2$) is a material of great significance in traditional as well as in advanced ceramics. It can be elaborated either by sol–gel methods [5–9] that are generally expensive or by combustion synthesis [10,11] or more classically from raw materials such as clays, kaolin and alumina which are abundant and low-cost. Kaolinite ($Al_2O_3{\cdot}2SiO_2{\cdot}2H_2O$) is a very advantageous mineral for mullite synthesis. Because of a higher silica content in kaolinite than in mullite, an addition of alumina is theoretically enough to make stoichiometric mullite. This enrichment is generally done by alumina [12–18] or aluminum hydroxide [19–23] additions. Although raw materials are not very expensive, the synthesis of mullite from these minerals requires high temperatures (1500–1600 °C) and a long heat treatment. The synthesis processes use a lot of energy which increases the cost of products.

The SHS synthesis, of which Merzhanov [24] was a precursor, has the advantage of saving energy and producing porous bodies. Indeed, after a local ignition of the synthesis reaction at low temperature, the reaction becomes self-propagating thanks to the heat released by its own exothermicity. This kind of synthesis is largely used for production of intermetallic compounds [25,26], carbides [27] and oxides [28]. To our knowledge this has not yet been used for mullite synthesis.

Porous refractory materials with high-temperature application are of great interest today (insulators, catalyst supports, filters and so on). They can be produced by various techniques as stated in a previous paper [29] in which we showed that porosity was created by aluminum oxidation, as Ebadzadeh [30] observed before us in mullite–zirconia composites.

In order to produce mullite, several authors [31–34] have successfully used aluminum powder additions. We have chosen this synthesis method to produce porous mullite bodies starting from kaolinitic clay. The exothermicity of aluminum oxidation reaction in an oxygen atmosphere could be used to ignite a self-propagating high-temperature synthesis (SHS). Moreover, because MgO is well-known for stimulating both the formation and sintering of mullite [4,17,35,36] and since the aluminum powder is generally superficially oxidized, magnesium metal powder will be mixed with a clay/aluminum mixture in order to test its effect on the ignition of SHS reaction, the generation of mullite and the consolidation of bodies at the same time.

* Corresponding author. Tel.: +33 555457487; fax: +33 555457586.
E-mail address: francoise.nardou@unilim.fr (F. Nardou).

0272-8842/$36.00 © 2009 Published by Elsevier Ltd and Techna Group S.r.l.
doi:10.1016/j.ceramint.2009.07.025

2. Experimental procedure

The characteristics of the kaolinitic clay powder were already given in a previous work [29] and its chemical composition can be seen in Table 1. SHS treatments need exothermic reactions with a very high energy release; the dehydroxylation of kaolinite that occurs near 600 °C is an endothermic effect as opposed to the exothermic oxidation of the Al and Mg metal powders. In order to prevent this effect, the kaolin powders were subjected to a first low temperature calcination. A batch of kaolinite is prepared by dry ball-milling the clay for 3 h using alumina balls. The powder obtained in this way was then heat treated at 650 °C for 1 h so as to provoke the dehydroxylation.

Aluminum powder (purity 99%, average grain size <45 μm) is provided by CERAC and magnesium powder (purity 98%, average grain size <250 μm) by VWR International.

Three 50 g batches named A, B, and C were prepared by mixing 89.5 wt.% of clay pre-treated at 650 °C and 10.5 wt.% of aluminum powder with various small amounts of magnesium powder (A:0, B:0.5, and C:1.5 g) in order to obtain 0 or about 1 or 3 wt.% of magnesium. The different batches were ground for 13 h in ethanol using a FRITSCH planetary ball-mill (pulverisette 6) at 280 rpm. The powders were then dried at 100 °C for 24 h.

Cylindrical samples were processed using both uniaxial and isostatic pressing at about 200 MPa (average green density: 1.50 g/cm^3). These green compacts were then heated either as in a traditional reaction sintering or as in a SHS sintering. For reactive sintering we used a NABERTHERM LHT 04/17 furnace. The firing was carried out in air with a heating rate of 5 °C/min up to 1100 °C and then of 10 °C/min to the dwell temperature (1400–1550 °C) that was maintained for 5 h before cooling to room temperature. For the SHS method the synthesis reaction occurred in an oxygen atmosphere inside a special device described elsewhere [37]. In this last method the reaction was locally ignited at about 600 °C on the upper surface of pellets by an electric oven.

The thermal behavior of various mixtures of clay and metallic powders were tested either in air or under flowing oxygen at a heating rate of 10 °C/min using differential thermal analysis (DTA) on a SETARAM type Labsys™ device. The thermal expansion of square section bar (0.5 cm × 0.5 cm × 2 cm) samples shaped by uniaxial pressing (100 MPa) was carried out in air on a LINSEIS, type L75 dilatometer. The identification of crystalline phases was done on a X-ray diffraction device (SIEMENS D 5000) using Cu Kα radiation. The morphology of both powders and sintered bodies, polished and thermally etched, was investigated by scanning electron microscopy (SEM) with a PHILIPS XL30 equipment working at 20 kV.

The bulk densities of the sintered pellets were evaluated by geometrical measurements. Archimedes' method was only used for the samples shaped by isostatic pressing. The percentage of porosity for samples sintered at 1550 °C for 5 h was determined using the following equation:

$$\%\,\text{porosity} = \frac{V_P - V_M}{V_P} \times 100$$

where V_P was the volume of pellets obtained by geometrical measurements and V_M the volume of mullite deduced from the weight of pellets (m_P) and the theoretical density of mullite ($d_M = 3.17$):

$$V_M = \frac{m_P}{d_M}$$

Table 1
Chemical composition of raw clay used (wt.%).

L.o.i.	SiO_2	Al_2O_3	Fe_2O_3	TiO_2	CaO	MgO	K_2O
12.23	51.32	30.77	1.93	1.76	0.06	0.03	0.10

3. Results and discussion

3.1. Thermal evolution of the different mixtures

3.1.1. In static air

In a preceding work [29] we studied, both the thermal behavior of raw kaolinitic clay and a mixture of raw clay/aluminum powder in static air. In the latter case we noted a shift of the thermal phenomena towards low temperatures as dehydroxylation occurred at 560 °C instead of 602 °C for pure kaolinite. The exothermic transformation which is controversially attributed to the formation of mullite 2:1 nuclei and/or spinel (γ-Al_2O_3 solid solution) from metakaolin by different authors [2,15,18,19] appeared at 959 °C instead of 974 °C.

In this work, a low temperature pre-fired kaolinite is used (Fig. 1A) and the endothermic peak of dehydroxylation is not visible of course. So, the pre-treated clay will be considered as metakaolin.

3.1.1.1. Mixture without Mg. When the batch A is heated (Fig. 1A), the first observed reaction is aluminum oxidation (around 570 °C) then followed by aluminum melting (660 °C). Simultaneously aluminum can reduce SiO_2 according to the reaction:

$$2Al + \tfrac{3}{2}SiO_2 \rightarrow \tfrac{3}{2}Si + Al_2O_3 \quad (1)$$

The transformation of metakaolin between 900 and 1000 °C is less defined and appears as a broad peak including probable oxidation of liquid aluminum which continues in the same temperature range. At higher temperature (960 °C) we can observe another exothermic effect that can be attributed to the transformation of metakaolin.

3.1.1.2. Mixtures with Mg. When magnesium powder is present in the mixture (batches B and C) the exothermic effect occurring near 600 °C (Fig. 1B and C) is enhanced compared to batch A. It increases and extends with Mg content.

Several reactions can occur at this temperature but, henceforth, formation of an Al–Mg alloy can be excluded because of the oxidizing operating in which all magnesium powder reacted explosively.

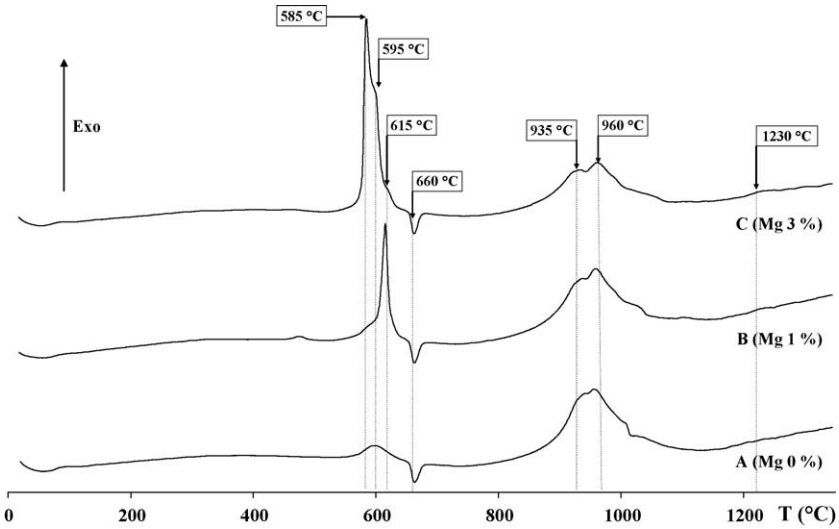

Fig. 1. DTA curves recorded in air on calcined clay/aluminum powder mixtures containing various amounts of magnesium powder.

The first two reactions to be considered concern the direct oxidation of metallic powders:

$$Mg + \tfrac{1}{2}O_2 \rightarrow MgO \quad (2)$$

$$2Al + \tfrac{3}{2}O_2 \rightarrow Al_2O_3. \quad (3)$$

Nevertheless aluminum/oxygen and magnesium/oxygen are two very different systems because:

- Al develops a protective layer of Al_2O_3 not only before its melting point (T_m = 660 °C) but also over T_m when Al is in the liquid state,
- in the opposite Mg oxidizes in a very short time (like an explosive reaction) and transforms into a non-protective MgO phase because the Pilling and Bedworth coefficient of Mg/MgO is lower than 1. Thus the complete oxidation of Mg takes place before the melting point of Mg (T_m = 651 °C).

So the addition of Mg brings a high heat flux to the B and C mixtures and involves an interaction between the two metallic oxidations. As it can be shown in Fig. 1, the temperatures of Mg and Al oxidation are shifted. Nevertheless the Al melting point always appears at 660 ± 1 °C while the exothermic reaction of magnesium oxidation occurs between 580 and 610 °C according to the experimental conditions.

The other reactions due to the presence of Mg in batches B and C are relative to the interaction of these same metallic powders with free silica or with silica component part of kaolinite:

$$2Mg + SiO_2 \rightarrow Si + 2MgO \quad (4)$$

$$2Al + \tfrac{3}{2}SiO_2 \rightarrow \tfrac{3}{2}Si + Al_2O_3 \quad (5)$$

as it had been observed by Tsunekawa et al. for metal matrix composites [38] and by Smith et al. for Al/Mg alloys [39]. Metallic Mg can also react with alumina [39,40] as

$$3Mg + Al_2O_3 \rightarrow 3MgO + 2Al \quad (6)$$

In order to confirm the occurrence of all these reactions (from (1) to (6)), a pelletized sample containing 3% of Mg was heat treated at 800 °C then quenched in air at room temperature. Fig. 2 shows the presence of metallic Al and Si, SiO_2 (quartz), TiO_2 (anatase) initially contained in the clay, MgO and even α-Al_2O_3, which is surprising because the crystallization of α-alumina regularly occurs at higher temperature (>1000 °C). Moreover the composition of thermal evolution (Fig. 3) of pure aluminum powder on the one hand and of pre-heated clay with 3 wt.% of Mg on the other hand suggests that the oxidation of Al naturally coated with amorphous Al_2O_3 starts about 550 °C. Mg oxidation also occurs near 600 °C (Fig. 3) with a strong exothermicity which increases the temperature of the sample and must enhance Al oxidation. Because of the low thermal conductivity of the ceramic and of the small diffusivity of oxygen through pores, the sample core very quickly shows the highest temperature and the lowest oxygen pressure such that Al and Mg can reduce silica contained in the kaolinite as

$$xAl/yMg + Al_2O_3{\cdot}2SiO_2 \rightarrow (1+x)Al_2O_3 + (x+y)Si + yMgO + 2 - (x+y)SiO_2 \quad (7)$$

This reaction leads to the formation of the corundum phase and could explain how α-Al_2O_3 may begin to crystallize about 700 °C whereas it is known to crystallize only over 1100–1200 °C.

At higher temperature (960 °C) we observed an exothermic effect (Fig. 1A) corresponding to the transformation of metakaolin. When magnesium is present (Fig. 1 B and C) a second exothermic peak clearly appears at 935 °C. It could be allotted either to liquid aluminum oxidation or to the formation of spinel [38,39] following the reaction:

$$MgO + Al_2O_3 \rightarrow MgAl_2O_4. \quad (8)$$

This hypothesis should result in an exothermic effect as observed by Tsunekawa et al. [38] at 775 °C for a mixture of SiO_2/Al/Mg powder, but in our work no spinel phase was

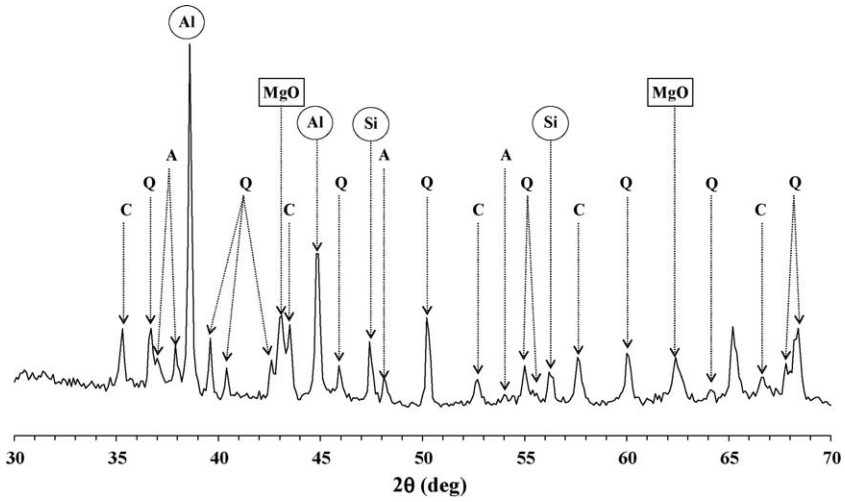

Fig. 2. X-ray pattern of a mixture calcined clay/10.5% Al/3% Mg heat treated at 800 °C and rapidly quenched in air to room temperature showing the presence of MgO. Al = aluminum, Si = silicon, C = corundum, Q = quartz, and A = anatase.

confirmed by XRD analysis on pellets quenched at 800, 900, or 1000 °C. Mg-spinel was only detected at higher temperature on quenched samples heat treated at 1200 °C (Fig. 4).

Undoubtedly due to its very low magnitude, the thermal peak of DTA analysis (Fig. 1) related to the crystallization of mullite and approximately localized at 1240 °C for pure clay disappears completely on DTA plots when the sample contains Mg. Nevertheless, this reaction is well visible by dilatometry as we will see further (Section 3.2), and, at the very most, one can guess it about 1230 °C.

3.1.2. *In flowing oxygen*

For batch A (without Mg), the oxidation of aluminum still begins about 600 °C in solid state even if the thermal phenomenon is smaller and extended (Fig. 5A, batch A). Beyond 660 °C, the aluminum in liquid state oxidizes very strongly at 944 °C. Contrary to that observed in static air the latter peak can offer the opportunity to ignite an SHS reaction on batch A in flowing oxygen.

For batches B and C (containing Mg) only one well-defined peak appears about 600 °C but the peak temperature moves from 605 °C for B to 586 °C for batch C (Fig. 5B and C). This evolution reminds us of what is observed in static air (Section 3.1.1). In flowing oxygen, magnesium oxidation is complete at 586 °C (Fig. 5C) and is marked by a very sharp and significant exothermic effect, specific of an SHS reaction. Thus the exothermic peak of aluminum oxidation is masked. In Fig. 5C relative to batch C, we can see that this thermal effect is so intense that it interacts with the furnace temperature regulation and gives a loop shaped peak. In spite of this very strong exothermicity Al is not entirely oxidized since the peak corresponding to its melting always appears at 660 °C. At 955 °C one can note a last exothermic effect corresponding either to Al oxidation or/and to spinel formation (batches B and C).

3.2. *Traditional reactive sintering in air*

When magnesium is present, dilatometric analysis shows a swelling occurring at about 600 °C (Fig. 6B and C) which is not visible when there is no magnesium (Fig. 6A). In fact the origin of this swelling is the exothermicity of the magnesium oxidation which enhances the dilatation of Al and allows it to expand by cracking the alumina layer. This swelling is

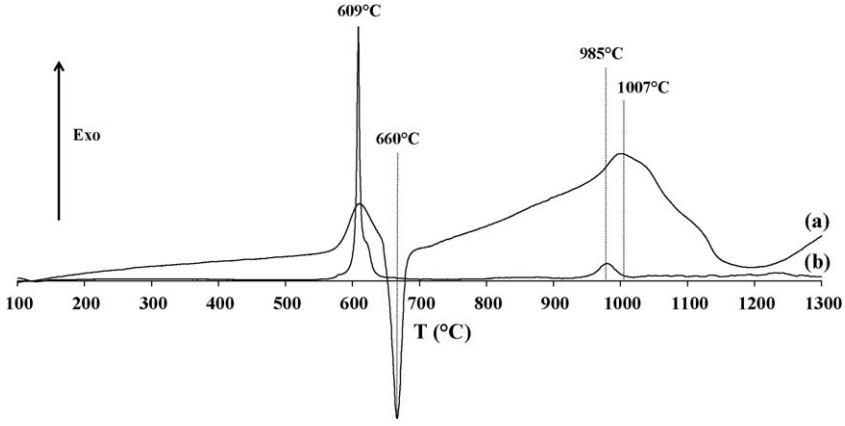

Fig. 3. DTA curves recorded in air of: (a) pure aluminum powder, (b) calcined clay with 3 wt.% of Mg.

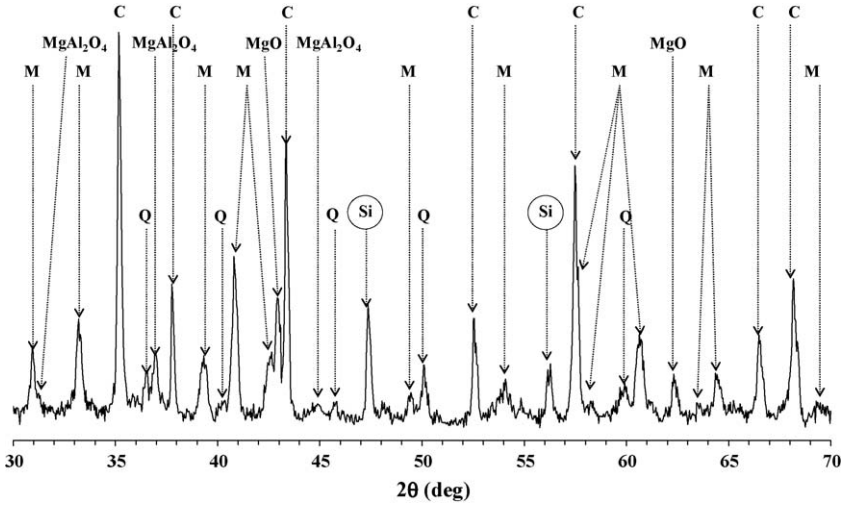

Fig. 4. X-ray pattern of a mixture calcined clay/10.5% Al/3% Mg heat treated at 1200 °C and rapidly quenched in air to room temperature showing the presence of $MgAl_2O_4$. Si = silicon, C = corundum, Q = quartz, and M = mullite.

maximum when the melting point of aluminum is attained. Because of the low thermal dilatation coefficient of the clay, this swelling cannot be also attributed to the expansion of kaolin. Then, a first shrinkage appears between 900 and 1000 °C and can be allotted to the formation of mullite 2:1 or spinel from metakaolin. The beginning of the crystallization of mullite phase occurs at about 1200 °C while a second shrinkage develops. So, the two transformations provoke a shrinkage when they take place. Thus, it can be assumed that the kinetics of sintering will be dependent on the rate of the transformation.

After sintering at 1550 °C for 5 h, mullite is found to be the only phase constituent of the samples that are characterized by:

- a yellowish color due to the presence of iron oxide in the initial clay (Table 1),
- a macroporosity increasing with the magnesium content (Fig. 7a).

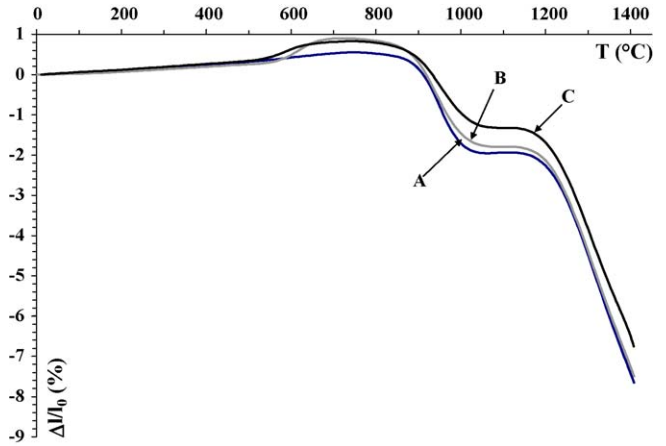

Fig. 6. Dilatometric analysis, taken in air, of square section bars shaped from the tree mixtures of powders (A: Mg 0%, B: Mg 1%, C: Mg 3%).

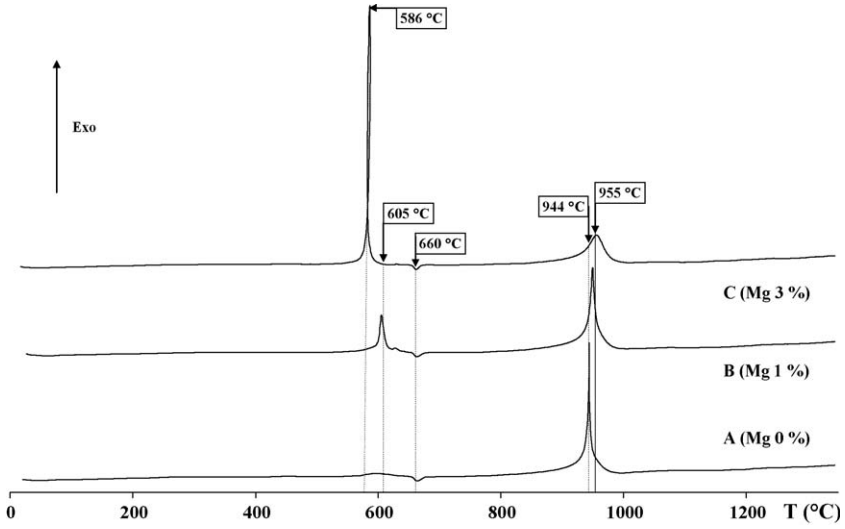

Fig. 5. DTA curves taken under flowing oxygen of calcined clay/aluminum powder mixtures containing various amounts of magnesium powder.

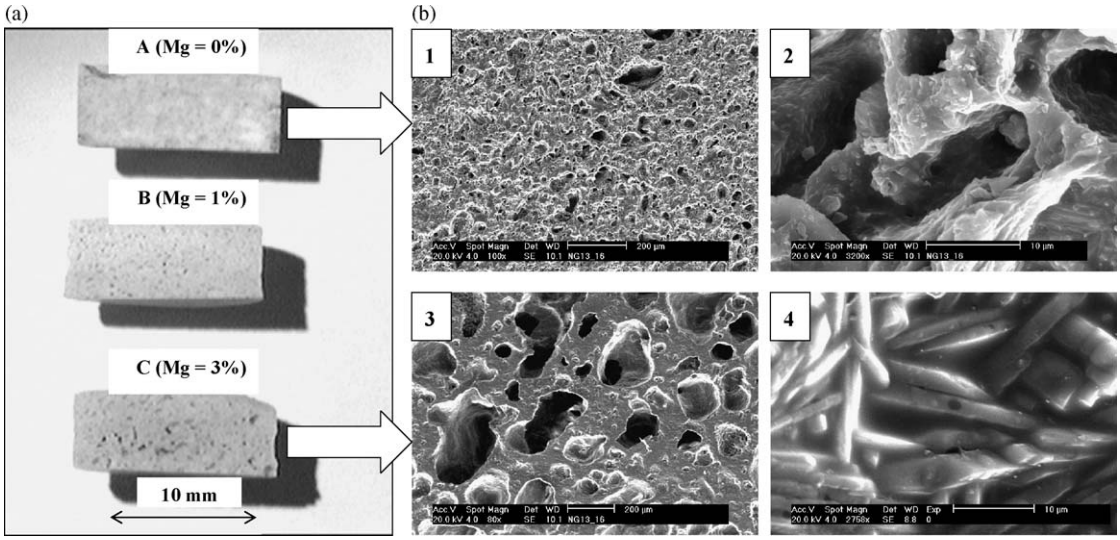

Fig. 7. Evolution of porosity with magnesium content after traditional sintering in air 5 h at 1550 °C. (a) Macrographs of cross-sections of different samples from mixtures A, B and C. (b) SEM micrographs of cross-sections showing: (1) and (2) a sample obtained from mixture A (Mg = 0 wt.%) (3) and (4), a sample obtained from mixture C (Mg = 3 wt.%).

In fact there are two types of porosity in the samples:

- a macroporosity visible without magnification (Fig. 7a),
- a microporosity shown by scanning electron microscopy observations (Fig. 7b).

The dimensions of this microporosity seem to be related to the particle sizes of the initial metallic powders. When there is no magnesium in the batch, microporosity sizes ∼45 μm which is of the order of aluminum particles. On the contrary samples containing magnesium present a binodal pore distribution with two dimensions close respectively to those of aluminum (∼45 μm) and magnesium grains (∼250 μm).

Moreover, needle shape crystallites of mullite have been revealed at higher magnification on SEM micrographs (Fig. 7b4). This aspect of needles is all the more marked than the magnesium content is higher.

Whatever the method of shaping used (uniaxial or isostatic pressing), the densities of the samples obtained after sintering (1550 °C, 5 h) are low and decrease with the magnesium content (Table 2). With addition of 3 wt.% of magnesium, porosity reaches a maximum value of 56% in volume. Nevertheless, in spite of their low density, the sintered bodies have a good mechanical cohesion.

Table 2
Densities of the different sintered bodies for 5 h at 1550 °C, shaped both by uniaxial and isostatic pressing.

Shaping	Density		Porosity (%)	
Shaping	Uniaxial	Isostatic	Uniaxial	Isostatic
Mixture A	2.21	2.36	30	25
Mixture B	1.76	1.95	45	38
Mixture C	1.64	1.36	48	56

3.3. Innovative SHS process in oxygen

The best experimental conditions to elaborate mullite by the innovative SHS process can be deduced from the thermal evolution of powders mixtures (cf. Section 3.1). From these results the SHS process can be ignited in oxygen atmosphere:

- either at relatively high-temperature (950 °C) with mixtures containing fired clay and aluminum powder (10.5 wt.%),
- or at lower temperature (∼600 °C) by adding magnesium powder (1–3%) to clay/aluminum 10.5 wt.% mixtures.

We choose to test the SHS process in flowing oxygen atmosphere and to study the behavior of the three batches A (without Mg), and B (1% Mg), and C (3% Mg). The SHS reactions were locally ignited at about 600 °C by heating up the upper surface of the pellet thanks to an electric furnace whose lower part is taken down close to the upper surface of the pellet. As soon as the reaction is initiated the furnace is withdrawn and the reaction front propagates quickly to the bottom of the sample.

After cooling the samples take on a black color (Fig. 8a) which can be explained by their structure as we will see later. Fig. 8a also shows some large cracks on the two samples. These cracks are due to the very high-temperature gradient which occurs during the SHS process whose cooling down step can be equivalent to a real quenching. Besides these large cracking zones more compact areas present a porosity which increases with Mg ratio as for the reactive sintering. SEM observations of cross-sections (Fig. 8b) show a vitreous aspect with interconnected porosities. The sizes of pores increase with the magnesium content but because of the thermal cycle of the SHS process (rise in temperature in a very short time) the microstructure is finer than that obtained with reactive

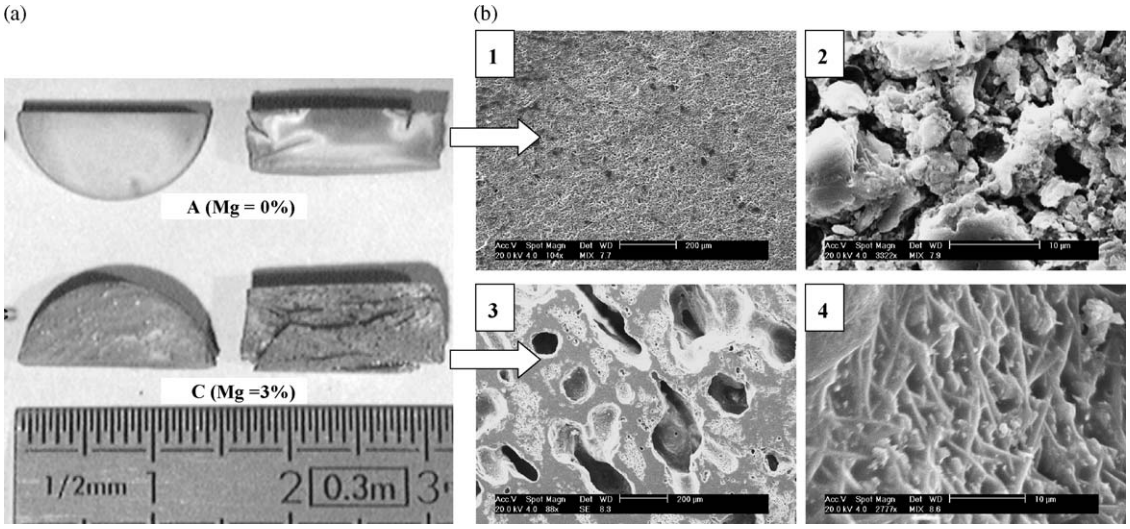

Fig. 8. Observations of samples from mixtures A (Mg = 0 wt.%) and C (3 wt.% Mg) after SHS reaction. (a) Macrographs of samples surfaces and cross-sections. (b) SEM micrographs of cross-sections showing: (1) and (2) a sample obtained from mixture A, (3) and (4) a sample obtained from mixture C.

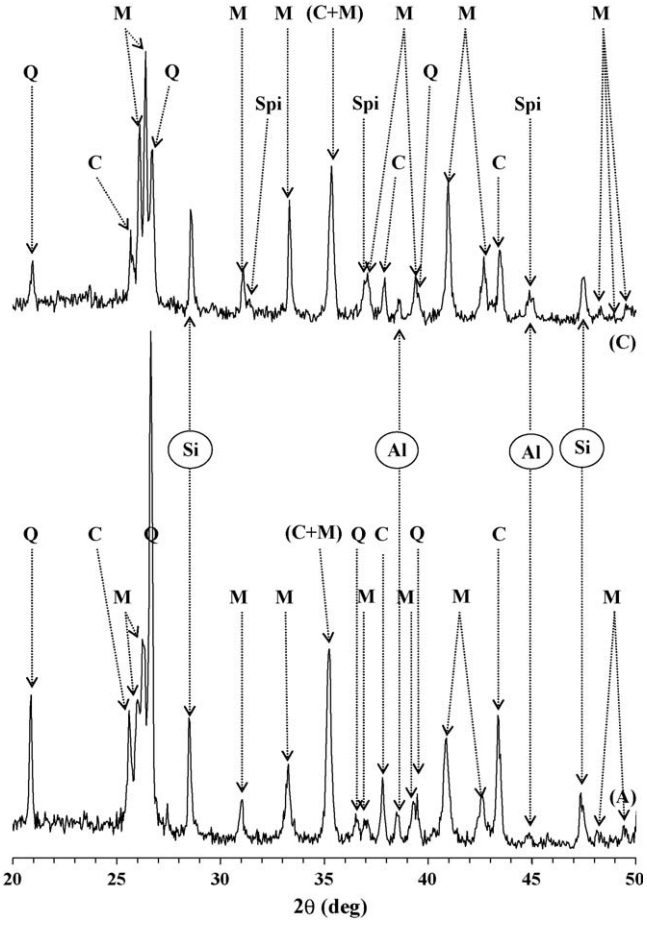

Fig. 9. XRD patterns of samples from mixtures A (0 wt.% Mg) and C (3 wt.% Mg) just after SHS treatment (Q = quartz, C = corundum, M = mullite, Spi = s-pinel, Al = aluminum, and Si = silicon).

sintering for example needles of mullite are very thin (Fig. 8b4).

The XRD analysis of powders coming from crushed samples containing respectively 0 and 3 wt.% of Mg (Fig. 9) enabled to identify mullite, quartz, α-alumina, and silicon metal (which blackened the sample) as significant phases with traces of aluminum metal. The presence of silicon shows that silica was partially reduced by aluminum and this in spite of the fact that the reaction takes place in flowing oxygen. This is the consequence of the formation of a vitreous phase on the periphery of the sample which constitutes a barrier to the diffusion of oxygen towards the core.

When the samples contain magnesium (Fig. 9, batch C) another additional phase appears which correspond to spinel ($MgAl_2O_4$). Moreover, the presence of magnesium in initial samples increases the ratio of mullite contained in the sample after SHS treatment. If one refers to bibliography [17,35,36] MgO is well known to stimulate the mullite formation and consequently MgO interacts with other phases during SHS process. The spinel phase ($MgAl_2O_4$), identified after SHS reaction in samples containing magnesium, comes from the following reaction:

$$MgO + Al_2O_3 \rightarrow MgAl_2O_4 \quad (9)$$

and thus probably reacts with metakaolin to form mullite.

Thus, after SHS heat treatment, the A, B and C pellets are composed of:

- metallic phases (Si and traces of Al),
- quartz,
- α-alumina,
- and spinel ($MgAl_2O_4$) when there is Mg,

in addition to mullite.

It means that all the reactions leading to the formation of mullite are not complete since the rest phases correspond to reactive phases not yet transformed into mullite.

This can be confirmed by applying a post-heat treatment to SHS treated samples (in air for 5 h at 1550 °C) identical to traditional reactive sintering (Section 3.2).

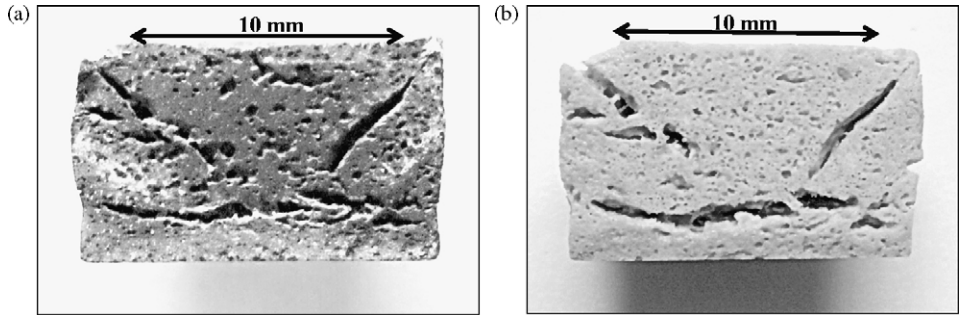

Fig. 10. Macrographs of cross-section of samples from mixture C with 3 wt.% of Mg: (a) just after SHS reaction, (b) after SHS reaction and post-heat treatment of 5 h at 1550 °C.

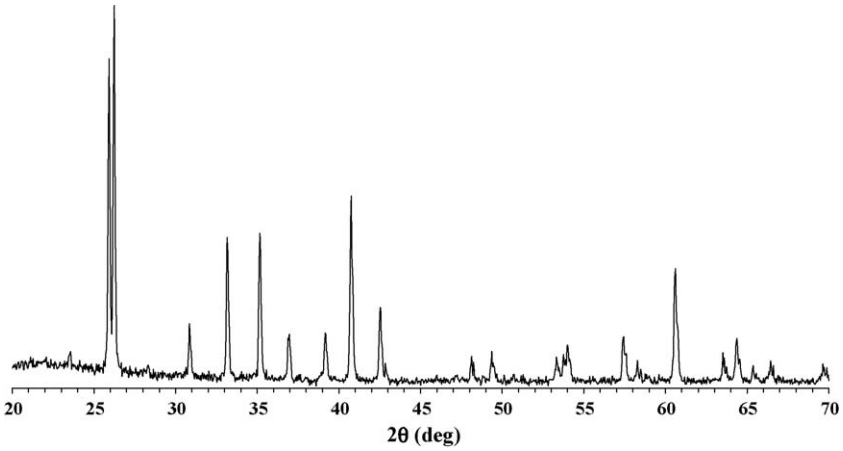

Fig. 11. XRD pattern of sample from mixture C (3 wt.% Mg) after SHS reaction and post-heat treatment of 5 h at 1550 °C. Only mullite is visible.

Indeed, after this post-treatment, SHS samples become yellow (Fig. 10) and mullite is now the only observed phase even when they contain 3 wt.% of Mg (Fig. 11).

It can be concluded that the highest temperature reached in the sample core during SHS process carried out in oxygen is not sufficient to obtain a total conversion of reactive and transitive phases in mullite even when the initial mixture contains 3 wt.% of magnesium.

4. Conclusion

The elaboration of pure porous mullite bodies can be effective with reactive sintering at 1550 °C from pressed mixtures of fired kaolinite with addition of aluminum and magnesium metallic powders.

The production of the same bodies with a more simple and economic SHS process has been explored. Production of pure mullite has not been obtained: some other phases (like Si and Al metallic phases, quartz, α-alumina and spinel) are present in addition to mullite phase.

An optimization of the process is planned, like the modification of grain size in reactive phases, in order to obtain only mullite phase.

Whatever the process applied to kaolinite and metallic mixtures, the porosity size of the pressed bodies after heat treatment seems to be in relation with the grain size of the initial metal powders and the porosity volume with the magnesium content. Then, the metal powders granulometry and content can probably monitor the porosity.

References

[1] H. Schneider, Thermal expansion of mullite, J. Am. Ceram. Soc. 73 (7) (1990) 2073–2076.
[2] V. Viswabaskaran, F.D. Gnanam, M. Balasubramanian, Mullitisation behaviour of calcined clay-alumina mixtures, Ceram. Int. 29 (5) (2003) 561–571.
[3] D.G. Goski, W.F. Caley, Reaction sintering of kyanite and alumina to form mullite composites, Can. Metal. Quart. 38 (2) (1999) 119–126.
[4] L. Montanaro, J.M. Tulliani, C. Perrot, A. Negro, Sintering of industrial mullites, J. Eur. Ceram. Soc. 17 (14) (1997) 1715–1723.
[5] J. Ossaka, Tetragonal mullite-like phase from co-precipitated gels, Nature 191 (4792) (1961) 1000–1001.
[6] F. Cluzel, G. Larnac, J. Phalippou, Structure and thermal evolution of mullite aerogels, J. Mater. Sci. 26 (22) (1991) 5979–5984.
[7] J.S. Lee, S.C. Yu, Characteristics of mullite prepared from co-precipitated $3Al_2O_3$–$2SiO_2$ powders, J. Mater. Sci. 27 (19) (1992) 5203–5208.
[8] E. Ruiz de Sola, F.J. Torres, J. Alarcón, Thermal evolution and structural study of 2:1 mullite from monophasic gels, J. Eur. Ceram. Soc. 26 (12) (2006) 2279–2284.
[9] S. Ding, Y.-P. Zeng, D. Jiang, Fabrication of mullite ceramics with ultrahigh porosity by gel freeze drying, J. Am. Ceram. Soc. 90 (7) (2007) 2276–2279.
[10] R. Gopi Chandran, K.C. Patil, A rapid combustion process for the preparation of crystalline mullite powders, Mater. Lett. 10 (6) (1990) 291–295.
[11] O. Burgos-Montes, R. Moreno, Colloidal behaviour of mullite powders produced by combustion synthesis, J. Eur. Ceram. Soc. 27 (16) (2007) 4751–4757.

[12] J. Temuujin, K.J.D. MacKenzie, M. Schmücker, H. Schneider, J. McManus, S. Wimperis, Phase evolution in mechanically treated mixtures of kaolinite and alumina hydrates (gibbsite and boehmite), J. Eur. Ceram. Soc. 20 (4) (2000) 413–421.
[13] M.A. Sainz, F.J. Serrano, J.M. Amigo, J. Bastida, A. Caballero, XRD microstructural analysis of mullites obtained from kaolinite-alumina mixtures, J. Eur. Ceram. Soc. 20 (4) (2000) 403–412.
[14] C.Y. Chen, G.S. Lan, W.H. Tuan, Preparation of mullite by the reaction sintering of kaolinite and alumina, J. Eur. Ceram. Soc. 20 (14–15) (2000) 2519–2525.
[15] V. Viswabaskaran, F.D. Gnanam, M. Balasubramanian, Mullite from clay–reactive alumina for insulating substrate application, Appl. Clay Sci. 25 (1–2) (2004) 29–35.
[16] Y.-F. Chen, M.-C. Wang, M.-H. Hon, Kinetics of secondary mullite formation in kaolin–Al_2O_3 ceramics, Scr. Mater. 51 (3) (2004) 231–235.
[17] M. Heraiz, A. Merrouche, N. Saheb, Effect of MgO addition and sintering parameters on mullite formation through reaction sintering kaolin and alumina, advances, Appl. Ceram. 105 (6) (2006) 285–290.
[18] F. Sahnoune, M. Chegaar, N. Saheb, P. Goeuriot, F. Valdivieso, Algerian kaolinite used for mullite formation, Appl. Clay Sci. 38 (3–4) (2008) 304–310.
[19] J. Pascual, j. Zapatero, M.C. Jiménez de Haro, I. Varona, A. Justo, J.L. Pérez-Rodríguez, P.J. Sánchez-Soto, Porous mullite and mullite-based composites by chemical processing of kaolinite and aluminium metal wastes, J. Mater. Chem. 10 (6) (2000) 1409–1414.
[20] Y.-F. Liu, X.-Q. Liu, S.-W. Tao, G.-Y. Meng, O.T. Sorensen, Kinetics of the reactive sintering of kaolinite-aluminum hydroxyde extrudate, Ceram. Int. 28 (5) (2002) 479–486.
[21] N.K. Mitra, A. Mandal, S. Maitra, A. Basumajumdar, Effect of TiO_2 on the interaction of dehydroxylated kaolinite with $Al(OH)_3$ gel in relation to mullitisation, Ceram. Int. 28 (3) (2002) 235–243.
[22] S. Li, N. Li, Effects of composition and temperature on porosity and pore size distribution of porous ceramics prepared from $Al(OH)_3$ and kaolinite gangue, Ceram. Int. 33 (4) (2007) 551–556.
[23] G. Chen, H. Qi, W. Xing, N. Xu, Direct preparation of macroporous mullite supports for membranes by in situ reaction sintering, J. Membr. Sci. 318 (1–2) (2008) 38–44.
[24] A.G. Merzhanov, The chemistry of self-propagating high-temperature synthesis, J. Mater. Chem. 14 (12) (2004) 1779–1786.
[25] K. Morsi, Review: reaction synthesis processing of Ni–Al intermetallic materials, Mater. Sci. Eng. A 299 (1–2) (2001) 1–15.
[26] D. Tingaud, F. Nardou, Influence of non-reactive particles on the microstructure of NiAl and NiAl–ZrO_2 processed by thermal explosion, Intermetallics 16 (5) (2008) 732–737.
[27] I.P. Borovinskaya, T.I. Ignat'eva, O.M. Emel'yanova, V.I. Vershinnikov, V.N. Semenova, Self-propagating high-temperature synthesis of ultrafine and nanometer-sized TiC particles, Inorg. Mater. 43 (11) (2007) 1206–1214.
[28] E.C. Partington, P. Grieveson, B. Terry, Self-sustaining oxidation of liquid aluminium and its alloys containing magnesium and silicon, J. Mater. Sci. 33 (9) (1998) 2447–2455.
[29] A. Esharghawi, C. Penot, F. Nardou, Contribution to porous mullite synthesis from clays by adding Mg and Al powders, J. Eur. Ceram. Soc. 29 (1) (2009) 31–38.
[30] T. Ebadzadeh, Porous mullite–ZrO_2 composites from reaction sintering of zircon and aluminum, Ceram. Int. 31 (8) (2005) 1091–1095.
[31] H. Balmori-Ramírez, E. Rocha-Rangel, E. Refugio-García, R.C. Bradt, Dense mullite from attrition-milled kyanite and aluminum metal, J. Am. Ceram. Soc. 87 (1) (2004) 144–146.
[32] J. Anggono, B. Derby, Mullite formation from the pyrolysis of aluminium-loaded polymethylsiloxanes: the influence of aluminium powder characteristics, J. Eur. Ceram. Soc. 26 (7) (2006) 1107–1119.
[33] A. Khabas, O.V. Nevvonen, V.I. Vereshchagin, Synthesis of mullite in the presence of nanodisperse aluminium powder, Refract. Ind. Ceram. 46 (1) (2005) 71–75.
[34] S. Li, J. Liu, Z. Li, W. Fan, P. Zhang, Microstructure and mechanical properties of mullite composites via pressure molding and by oxidation of an Al–Si alloy powder, key Eng. Mater., 368–372 (PART 1) 815–817.
[35] V. Viswabaskaran, F.D. Gnanam, Effect of MgO on mullitisation behavior of clays, J. Mater. Sci. Lett. 22 (9) (2003) 663–668.
[36] L.B. Kong, Y.Z. Chen, T.S. Zhang, J. Ma, F. Boey, H. Huang, Effect of alkaline-earth oxides on phase formation and morphology development of mullite ceramics, Ceram. Int. 30 (7) (2004) 1319–1323.
[37] D. Tingaud, C. Penot, F. Nardou, In situ monitoring of the kinetics of solid-gas SHS reaction: application to the Zr–O_2 system, Int. J. S. H. S. 16 (3) (2007) 110–118.
[38] Y. Tsunekawa, H. Suzuki, Y. Genma, Application of ultrasonic vibration to in situ MMC process by electromagnetic melt stirring, Mater. Design 22 (6) (2001) 467–472.
[39] G.W. Smith, W.J. Baxter, A.K. Sachdev, A calorimetric investigation of fiber/matrix reaction in fiber-reinforced aluminium alloy 339, Mater. Sci. Eng. A 284 (1–2) (2000) 246–253.
[40] P. Pascal, Nouveau traité de chimie minérale, Masson, Paris, 1962, tome IV, 150.